

SUPPLEMENTARY INFORMATION

Impaired Plakophilin-2 in obesity breaks cell cycle dynamics to breed adipocyte senescence

Aina Lluch^{1,2}, Jessica Latorre^{1,2}, Angela Serena-Maione³, Isabel Espadas⁴, Estefanía Caballano-Infantes^{1,2}, José M. Moreno-Navarrete^{1,2}, Núria Oliveras-Cañellas^{1,2}, Wifredo Ricart^{1,2}, María M. Malagón^{2,5}, Alejandro Martin-Montalvo⁴, Walter Birchmeier⁶, Witold Szymanski⁷, Johannes Graumann⁷, María Gómez-Serrano⁸, Elena Sommariva³, José M. Fernández-Real^{1,2,9,10}, Francisco J. Ortega^{1,2,10*}

¹ Department of Diabetes, Endocrinology and Nutrition, Institut d'Investigació Biomèdica de Girona (IDIBGI), Girona (Spain).

² CIBER de la Fisiopatología de la Obesidad y la Nutrición (CIBEROBN), Instituto de Salud Carlos III (ISCIII), Madrid (Spain).

³ Unit of Vascular Biology and Regenerative Medicine, Centro Cardiologico Monzino IRCCS, Milan (Italy).

⁴ Centro Andaluz de Biología Molecular y Medicina Regenerativa (CABIMER), Consejo Superior de Investigaciones Científicas (CSIC), University Pablo de Olavide, Seville (Spain).

⁵ Department of Cell Biology, Physiology and Immunology, Instituto Maimonides de Investigación Biomédica de Córdoba (IMIBIC), University of Córdoba, Reina Sofia University Hospital, Córdoba (Spain).

⁶ Max Delbrück Center for Molecular Medicine, Berlin-Buch (Germany).

⁷ Institute of Translational Proteomics, Biochemical/Pharmacological Centre, Philipps University, Marburg (Germany).

⁸ Institute for Tumor Immunology, Center for Tumor Biology and Immunology, Philipps University, Marburg (Germany)

⁹ Department of Medical Sciences, School of Medicine, University of Girona (Spain).

¹⁰ These authors jointly supervised this work.

*Corresponding author:

Francisco J. Ortega. Email: fortega@idibgi.org

Short title: Relevance of Plakophilin-2 in adipocytes.

SUPPLEMENTARY TABLES

Supplementary Table S1. Anthropometric and biochemical data of 24 health-weight age-matched women selected as a reference group (controls) for cross-sectional comparisons, and 20 obese women before (baseline) and ~2 years after bariatric surgery (post-weight loss). See also in [Figure 2b](#).

Study variables	Controls (n=24)	Obese baseline (n=20)	Obese post-weight loss	p-value ^a	p-value ^b
Age (years)	45 ± 5	49 ± 9	51 ± 9	0.105	<0.0001
BMI (kg/m ²)	24.4 ± 2.9	43.1 ± 5	29.2 ± 5.5	<0.0001	<0.0001
Fat mass (%)	38.6 ± 5	56.1 ± 7.4	40.1 ± 7.4	<0.0001	<0.0001
SBP (mmHg)	116.4 ± 13.7	128.8 ± 13.7	130.7 ± 16.9	0.003	0.215
DBP (mmHg)	70.8 ± 12.2	79 ± 9.7	74.2 ± 12.6	0.014	0.089
Glucose (mg/dl)	89.6 ± 9.5	94.5 ± 14	87.4 ± 13.5	0.162	0.018
HbA1c (%)	5.4 ± 0.3	5.5 ± 0.6	5.3 ± 0.3	0.466	0.261
Cholesterol (mg/dl)	188.1 ± 35.9	183.1 ± 33.6	184.7 ± 51.8	0.624	0.851
LDL (mg/dl)	111.4 ± 31.8	105.1 ± 28.8	100.4 ± 29.7	0.477	0.407
HDL (mg/dl)	58.8 ± 13.2	56.5 ± 13.1	73.8 ± 22.1	0.547	<0.0001
Triglycerides (mg/dl)	94.6 ± 46.3	107.9 ± 43.1	81.4 ± 28.7	0.31	0.006
PKP2 in SC	0.0197 ± 0.0213	0.0032 ± 0.0036	0.024 ± 0.0183	<0.0001	<0.0001

Values represent mean ± S.D. BMI: body mass index, S/DBP: systolic/diastolic blood pressure, HbA1c: glycated haemoglobin, L/HDL: low/high density proteins, PKP2: Plakophilin-2, SC: subcutaneous adipose tissue. ^aResults in controls (BMI<30 kg/m²) versus severe obese (BMI≥35 kg/m²) women (baseline) were compared by two-tailed Fisher's exact t-test. ^bResults post-weight loss versus baseline were compared by paired t-test.

Supplementary Table S2. Characteristics of study subjects, including gene expression measures taken in depths of subcutaneous and omental adipose tissue. See also in [Figures 2d](#) and [2f](#).

	NO with NGT	NO with IGT	Ob with NGT	Ob with IGT	ANOVA	p-value ^a	p-value ^b	p-value ^c
n (men/women)	19/77	3/8	18/53	8/34				
Age (years)	48 ± 10	55 ± 11	44 ± 11	46 ± 10	0.01	0.183	0.128	0.846
BMI (kg/m ²)	24.9 ± 3.5	27.8 ± 1.7	43.7 ± 7.5	45.1 ± 7.9	<0.0001	0.428	<0.0001	0.63
Fat mass (%)	33.4 ± 6.4	37.6 ± 6.4	54.4 ± 9.8	57.2 ± 11.7	<0.0001	0.437	<0.0001	0.382
SBP (mmHg)	123 ± 15	137 ± 19	135 ± 17	137 ± 21	<0.0001	0.047	<0.0001	0.95
DBP (mmHg)	73 ± 12	84 ± 8	80 ± 11	80 ± 11	<0.0001	0.02	0.002	1
Fasting glucose (mg/dl)	88.1 ± 8.8	137.7 ± 53.6	90.5 ± 8.8	123.9 ± 40.1	<0.0001	<0.0001	0.905	<0.0001
Hb1Ac (%)	5.3 ± 0.41	7.21 ± 2.93	5.04 ± 0.48	5.67 ± 1.36	<0.0001	<0.0001	0.475	0.027
Cholesterol (mg/dl)	193.5 ± 40.2	239.8 ± 40.3	192.1 ± 38.2	185.8 ± 33.7	0.001	0.002	0.996	0.85
LDL (mg/dl)	113 ± 32.9	159.1 ± 34.2	114.9 ± 32.9	109.5 ± 32.2	<0.0001	<0.0001	0.985	0.872
HDL (mg/dl)	63.3 ± 20.2	48.4 ± 8.4	58.6 ± 42.7	50.6 ± 11.1	0.083	0.388	0.746	0.517
Triglycerides (mg/dl)	95.3 ± 45.8	174.5 ± 74.7	113.8 ± 69	138.4 ± 68.7	<0.0001	0.001	0.226	0.183
Gene expression in SC adipose tissue								
<i>PKP2</i>	0.0218 ± 0.0252	0.0084 ± 0.0067	0.0066 ± 0.008	0.0062 ± 0.0076	<0.0001	0.153	<0.0001	1
<i>LEP</i>	0.481 ± 0.309	0.816 ± 0.179	0.842 ± 0.367	0.944 ± 0.576	<0.0001	0.083	<0.0001	0.724
<i>HSD11B1</i>	0.0406 ± 0.0379	0.0573 ± 0.052	0.0729 ± 0.0447	0.0711 ± 0.0441	<0.0001	0.947	<0.0001	0.997
<i>SPP1</i>	0.0294 ± 0.064	0.0727 ± 0.05	0.0746 ± 0.0861	0.1198 ± 0.1907	0.006	0.886	0.169	0.235
<i>SLC27A2</i>	0.00193 ± 0.00324	0.00031 ± 0.00055	0.00022 ± 0.00066	0.00011 ± 0.00032	<0.0001	0.387	<0.0001	0.994
<i>FASN</i>	0.91 ± 0.859	0.299 ± 0.434	0.383 ± 0.664	0.144 ± 0.174	<0.0001	0.056	<0.0001	0.491
<i>TNF</i>	0.00238 ± 0.00263	0.00247 ± 0.00083	0.00316 ± 0.00209	0.00353 ± 0.00255	0.119	1	0.347	0.905
<i>TMEM26</i>	0.00062 ± 0.00074	0.00046 ± 0.00007	0.00068 ± 0.00083	0.00085 ± 0.00134	0.715	0.987	0.989	0.866
<i>NRG4</i>	0.00017 ± 0.00015	0.00013 ± 0.00009	0.00033 ± 0.00059	0.00047 ± 0.00133	0.351	1	0.679	0.843
Gene expression in OM adipose tissue								
<i>PKP2</i>	0.0245 ± 0.0247	0.0132 ± 0.0065	0.0266 ± 0.023	0.028 ± 0.0219	0.418	0.196	0.969	0.995
<i>LEP</i>	0.189 ± 0.162	0.322 ± 0.114	0.324 ± 0.193	0.256 ± 0.099	0.008	0.246	0.008	0.742
<i>HSD11B1</i>	0.0399 ± 0.0327	0.0899 ± 0.0788	0.0539 ± 0.0254	0.0502 ± 0.0276	0.027	0.091	0.099	0.946
<i>SPP1</i>	0.0382 ± 0.0483	0.1273 ± 0.1104	0.0581 ± 0.1153	0.0615 ± 0.0513	0.376	0.3	0.872	0.999
<i>SLC27A2</i>	0.00376 ± 0.00511	0.00023 ± 0.00018	0.00073 ± 0.00226	0.00067 ± 0.00184	0.004	0.198	0.004	1
<i>FASN</i>	0.541 ± 0.58	0.157 ± 0.099	0.101 ± 0.123	0.057 ± 0.056	<0.0001	0.034	<0.0001	0.954
<i>TNF</i>	0.00311 ± 0.00322	0.00192 ± 0.00161	0.00633 ± 0.00943	0.00537 ± 0.00293	0.04	0.953	0.052	0.948
<i>TMEM26</i>	0.00185 ± 0.00146	0.00198 ± 0.00166	0.00305 ± 0.00197	0.00289 ± 0.00166	0.004	0.998	0.004	0.98
<i>NRG4</i>	0.00223 ± 0.00262	0.0013 ± 0.00149	0.00375 ± 0.00257	0.00475 ± 0.00267	0.001	0.961	0.034	0.367

Values represent mean ± S.D. NO/Ob: non-obese/obese participants, N/IGT: normal/impaired glucose tolerance, BMI: body mass index, S/DBP: systolic/diastolic blood pressure, HbA1c: glycated haemoglobin, L/HDL: low/high density proteins, SC/OM: subcutaneous/omental, *PKP2*: plakophilin-2, *LEP*: leptin, *HSD11B1*: hydroxysteroid 11-beta dehydrogenase 1, *SPP1*: secreted phosphoprotein 1 (aka osteopontin), *SLC27A2*: solute carrier family 27 member 2, *FASN*: fatty acid synthase, *TNF*: tumor necrosis factor, *TMEM26*: transmembrane protein 26, *NRG4*: neuregulin-4. One-way ANOVA was followed by Tukey's honestly significant difference (HSD) post-hoc test for ^anon-obese subjects with and without IGT, ^bnon-obese participants *versus* obese subjects without IGT, and ^cobese participants with and without IGT. Obesity was set at BMI ≥ 30 kg/m². IGT was defined as impaired fasting glucose (≥ 110 mg/dl), and/or HbA1c of ≥ 5.7%.

Supplementary Table S3. Spearman's rho tests for correlations between study variables and measures of *PKP2* gene expression taken in bulk subcutaneous and omental adipose tissue. See also in [Figures 2e](#) and [2g](#), and in [Supplementary Figures S2f-i](#).

Correlations	<i>PKP2</i> in OM (n=131)		<i>PKP2</i> in SC (n=183)	
	r	p	r	p
Age (years)	-0.28	0.001	0.04	0.578
BMI (kg/m ²)	0.13	0.146	-0.49	<0.0001
Fat mass (%)	0.11	0.235	-0.48	<0.0001
SBP (mmHg)	-0.13	0.194	-0.19	0.014
DBP (mmHg)	-0.02	0.828	-0.11	0.186
Fasting glucose (mg/dl)	-0.17	0.062	-0.23	0.002
Hb1Ac (%)	-0.39	<0.0001	0.01	0.924
Cholesterol (mg/dl)	-0.26	0.005	-0.14	0.062
LDL (mg/dl)	-0.29	0.002	-0.1	0.214
HDL (mg/dl)	0.07	0.489	0.11	0.134
Triglycerides (mg/dl)	-0.15	0.106	-0.31	<0.0001
<i>LEP</i> in OM/SC	-0.35	0.002	-0.52	<0.0001
<i>SPP1</i> in OM/SC	-0.25	0.026	-0.45	<0.0001
<i>HSD11B1</i> in OM/SC	-0.32	0.001	-0.32	<0.0001
<i>SLC27A2</i> in OM/SC	0.29	0.007	0.51	<0.0001
<i>PKP2</i> in SC (n=90 paired samples)	0.06	0.544		

OM/SC: omental/subcutaneous, BMI: body mass index, S/DBP: systolic/diastolic blood pressure, HbA1c: glycated haemoglobin, L/HDL: low/high density proteins, *LEP*: leptin, *HSD11B1*: hydroxysteroid 11-beta dehydrogenase 1, *SPP1*: secreted phosphoprotein 1 (also known as osteopontin), *SLC27A2*: solute carrier family 27 member 2, *PKP2*: plakophilin-2.

Supplementary Table S4. Functional enrichment of proteins down (in blue; query size of 488) and upregulated (in red; 1,113) in si-PKP2 adipocytes (first) and preadipocytes (589 and 801, respectively; second table). Enrichment analyses were performed with g:Profiler (<https://biit.cs.ut.ee/gprofiler/gost>). Only relevant terms in the Gene Ontology (GO) database are listed below and spotlighted in **Supplemental Figure S5a-d**. Abundance changes affecting proteins annotated in categories of interest are represented in **Figure 4h**.

#	source	term_name	term_id	adjusted_p-value	term_size	intersection_size
1	GO:MF	protein binding	GO:0005515	2,11E-21	14881	447
2	GO:MF	catalytic activity	GO:0003824	5,84E-15	5758	227
3	GO:MF	enzyme regulator activity	GO:0030234	1,21E-03	1300	59
4	GO:MF	translation factor activity, RNA binding	GO:0008135	2,56E-03	99	12
5	GO:MF	single-stranded DNA helicase activity	GO:0017116	7,39E-03	23	6
6	GO:MF	linear malto-oligosaccharide phosphorylase activity	GO:0102250	7,54E-03	3	3
7	GO:MF	SHG alpha-glucan phosphorylase activity	GO:0102499	7,54E-03	3	3
8	GO:MF	glycogen phosphorylase activity	GO:0008184	7,54E-03	3	3
9	GO:MF	extracellular matrix structural constituent	GO:0005201	1,20E-02	174	15
10	GO:MF	P-type calcium transporter activity	GO:0005388	2,07E-02	9	4
11	GO:MF	structural constituent of postsynaptic actin cytoskeleton	GO:0098973	2,96E-02	4	3
12	GO:BP	organonitrogen compound metabolic process	GO:1901564	2,48E-15	6441	239
13	GO:BP	organelle organization	GO:0006996	8,19E-07	3608	137
14	GO:BP	cell cycle	GO:0007049	1,07E-06	1825	84
15	GO:BP	double-strand break repair via break-induced replication	GO:0000727	2,86E-04	12	6
16	GO:BP	regulation of DNA-templated DNA replication initiation	GO:0030174	1,46E-03	15	6
17	GO:BP	biological process involved in interspecies interaction between organisms	GO:0044419	2,00E-03	1752	72
18	GO:BP	mesenchyme migration	GO:0090131	3,32E-03	5	4
19	GO:BP	response to virus	GO:0009615	5,86E-03	403	26
20	GO:BP	actin filament-based process	GO:0030029	5,90E-03	817	41
21	GO:BP	cytoplasmic translational initiation	GO:0002183	7,16E-03	40	8
22	GO:BP	collagen metabolic process	GO:0032963	1,04E-02	103	12
23	GO:BP	DNA unwinding involved in DNA replication	GO:0006268	1,90E-02	22	6
24	GO:BP	locomotion	GO:0040011	2,01E-02	1365	57
25	GO:BP	cell motility	GO:0048870	2,28E-02	1705	67
26	GO:BP	non-membrane-bounded organelle assembly	GO:0140694	3,02E-02	389	24
27	GO:BP	growth	GO:0040007	3,12E-02	937	43
28	GO:CC	cytoplasm	GO:0005737	1,07E-34	12365	404
29	GO:CC	focal adhesion	GO:0005925	9,33E-11	425	38
30	GO:CC	MCM complex	GO:0042555	1,53E-05	11	6
31	GO:CC	collagen-containing extracellular matrix	GO:0062023	3,76E-05	430	29
32	GO:CC	supramolecular complex	GO:0099080	1,21E-04	1411	61
33	GO:CC	chromosomal region	GO:0098687	2,84E-04	396	26
34	GO:CC	midbody	GO:0030496	1,22E-03	207	17
35	GO:CC	MHC class I protein complex	GO:0042612	4,96E-03	8	4
36	GO:CC	cell division site	GO:0032153	1,04E-02	73	9
1	GO:MF	protein binding	GO:0005515	5,10E-40	14881	999
2	GO:MF	structural constituent of chromatin	GO:0030527	1,06E-14	101	33
3	GO:MF	catalytic activity	GO:0003824	2,26E-13	5758	439
4	GO:MF	structural constituent of cytoskeleton	GO:0005200	5,30E-11	109	30
5	GO:MF	P-type ion transporter activity	GO:0015662	4,39E-03	21	8
6	GO:MF	structural constituent of muscle	GO:0008307	7,56E-03	43	11
7	GO:MF	magnesium ion binding	GO:0000287	1,08E-02	227	29
8	GO:BP	organelle organization	GO:0006996	1,81E-27	3608	336
9	GO:BP	translation	GO:0006412	2,03E-17	745	104
10	GO:BP	ribosome biogenesis	GO:0042254	5,00E-10	312	51
11	GO:BP	organic acid metabolic process	GO:0006082	7,13E-09	979	103
12	GO:BP	nucleosome organization	GO:0034728	8,88E-08	143	30
13	GO:BP	cellular response to stress	GO:0033554	1,61E-07	1949	165
14	GO:BP	regulation of mRNA metabolic process	GO:1903311	5,01E-05	306	41
15	GO:BP	cellular respiration	GO:0045333	9,74E-05	244	35
16	GO:BP	regulation of cellular component biogenesis	GO:0044087	3,87E-04	971	88
17	GO:BP	cell morphogenesis	GO:0000902	3,60E-03	978	85
18	GO:BP	viral genome replication	GO:0019079	4,42E-03	126	21
19	GO:BP	viral release from host cell	GO:0019076	5,13E-03	31	10
20	GO:BP	regulation of binding	GO:0051098	8,33E-03	370	41
21	GO:BP	protein polymerization	GO:0051258	1,34E-02	287	34
22	GO:BP	response to hormone	GO:0009725	1,35E-02	875	76
23	GO:BP	axo-dendritic transport	GO:0008088	2,20E-02	78	15
24	GO:BP	intracellular signal transduction	GO:0035556	2,61E-02	2669	185
25	GO:BP	cell migration	GO:0016477	2,77E-02	1505	115
26	GO:BP	macromolecule modification	GO:0043412	4,00E-02	3840	251
27	GO:BP	system development	GO:0048731	4,39E-02	3987	259
28	GO:BP	cellular response to external stimulus	GO:0071496	4,57E-02	330	36
29	GO:CC	cytoplasm	GO:0005737	1,02E-83	12365	924

30	GO:CC	nucleosome	GO:0000786	2,60E-14	135	36
31	GO:CC	cytoplasmic stress granule	GO:0010494	1,75E-03	85	16
32	GO:CC	filopodium	GO:0030175	2,41E-03	107	18
33	GO:CC	preribosome	GO:0030684	8,86E-03	76	14
34	GO:CC	cytoplasmic side of membrane	GO:0098562	1,81E-02	207	25
35	GO:CC	polysome	GO:0005844	2,15E-02	72	13
36	GO:CC	myosin II filament	GO:0097513	4,96E-02	3	3

#	source	term_name	term_id	adjusted_p_value	term_size	intersection_size
1	GO:MF	catalytic activity	GO:0003824	6,13E-21	5758	281
2	GO:MF	protein binding	GO:0005515	7,04E-21	14881	530
3	GO:MF	P-type calcium transporter activity	GO:0005388	3,09E-07	9	7
4	GO:MF	structural constituent of cytoskeleton	GO:0005200	8,97E-06	109	17
5	GO:MF	double-stranded RNA binding	GO:0003725	1,43E-04	76	13
6	GO:MF	poly-purine tract binding	GO:0070717	1,02E-02	30	7
7	GO:MF	phenanthrene 9,10-monooxygenase activity	GO:0018636	1,29E-02	3	3
8	GO:MF	peptide antigen binding	GO:0042605	2,45E-02	34	7
9	GO:MF	alcohol dehydrogenase (NADP+) activity	GO:0008106	2,69E-02	24	6
10	GO:MF	poly(U) RNA binding	GO:0008266	3,45E-02	25	6
11	GO:BP	response to stress	GO:0006950	8,95E-25	4017	222
12	GO:BP	small molecule metabolic process	GO:0044281	2,19E-08	1865	102
13	GO:BP	phosphorus metabolic process	GO:0006793	4,07E-06	2788	128
14	GO:BP	organelle organization	GO:0006996	4,94E-04	3608	147
15	GO:BP	antigen proc. and pres. of exogenous peptide antigen via MHC class Ib	GO:0002477	1,33E-03	4	4
16	GO:BP	cell cycle	GO:0007049	2,14E-03	1825	85
17	GO:BP	cell development	GO:0048468	5,77E-03	2763	115
18	GO:BP	regulation of cardiac conduction	GO:1903779	8,39E-03	25	7
19	GO:BP	generation of precursor metabolites and energy	GO:0006091	1,81E-02	449	30
20	GO:BP	protection from natural killer cell mediated cytotoxicity	GO:0042270	1,91E-02	6	4
21	GO:BP	T cell mediated immunity	GO:0002456	1,97E-02	108	13
22	GO:BP	homeostatic process	GO:0042592	2,14E-02	1673	76
23	GO:BP	neurogenesis	GO:0022008	4,14E-02	1705	76
24	GO:CC	cytoplasm	GO:0005737	7,09E-58	12365	507
25	GO:CC	catalytic complex	GO:1902494	2,92E-07	1792	91
26	GO:CC	MHC class I protein complex	GO:0042612	2,80E-06	8	6
27	GO:CC	cytoskeleton	GO:0005856	9,07E-04	2412	100
28	GO:CC	NF-kappaB complex	GO:0071159	2,20E-03	6	4
29	GO:CC	I-kappaB/NF-kappaB complex	GO:0033256	2,29E-02	4	3
30	GO:CC	semaphorin receptor complex	GO:0002116	4,36E-02	11	4
31	GO:CC	membrane raft	GO:0045121	4,93E-02	324	21
1	GO:MF	protein binding	GO:0005515	1,31E-30	14881	724
2	GO:MF	extracellular matrix structural constituent	GO:0005201	2,46E-10	174	32
3	GO:MF	catalytic activity	GO:0003824	1,09E-09	5758	319
4	GO:MF	molecular adaptor activity	GO:0060090	1,65E-04	545	48
5	GO:MF	enzyme regulator activity	GO:0030234	7,84E-04	1300	87
6	GO:MF	peptidyl-lysine 5-dioxygenase activity	GO:0070815	1,83E-03	4	4
7	GO:MF	translation regulator activity	GO:0045182	1,14E-02	157	19
8	GO:MF	RNA binding	GO:0003723	1,31E-02	3113	167
9	GO:MF	heparin binding	GO:0008201	1,36E-02	173	20
10	GO:MF	phosphotransferase activity, carboxyl group as acceptor	GO:0016774	4,64E-02	3	3
11	GO:MF	protein kinase binding	GO:0019901	4,67E-02	709	50
12	GO:BP	organonitrogen compound metabolic process	GO:1901564	9,07E-23	6441	378
13	GO:BP	supramolecular fiber organization	GO:0097435	2,96E-18	819	92
14	GO:BP	ribosome biogenesis	GO:0042254	5,64E-13	312	47
15	GO:BP	basement membrane organization	GO:0071711	1,83E-04	38	11
16	GO:BP	Golgi vesicle transport	GO:0048193	1,28E-03	309	31
17	GO:BP	small molecule metabolic process	GO:0044281	2,84E-03	1865	109
18	GO:BP	Rap protein signal transduction	GO:0032486	7,74E-03	13	6
19	GO:BP	reg. of cysteine-type endopeptidase activity involved in apoptotic process	GO:0043281	1,60E-02	203	22
20	GO:BP	epithelial to mesenchymal transition	GO:0001837	1,96E-02	161	19
21	GO:BP	carbohydrate derivative metabolic process	GO:1901135	3,33E-02	1059	67
22	GO:CC	cytoplasm	GO:0005737	6,48E-63	12365	673
23	GO:CC	preribosome	GO:0030684	4,02E-06	76	16
24	GO:CC	myosin II filament	GO:0097513	1,71E-02	3	3

Supplementary Table S5. Characteristics of unrelated patients from which a subcutaneous fat biopsy was taken, during implantable cardioverter defibrillator implant, for the extraction of subcutaneous fat-derived stromal cells.

#	Patients	Age	Sex	Clinical diagnosis	Genetics
1	<i>PKP2</i> -1	27 years	W	ACM	<i>PKP2</i> c.2013delC p.Lys672ArgfsX12
2	<i>PKP2</i> -2	39 years	W	ACM	<i>PKP2</i> c.2013delC p.Lys672ArgfsX12
3	<i>PKP2</i> -3	24 years	M	ACM	<i>PKP2</i> c.121delG p.V406FfsX13
4	<i>PKP2</i> -4	42 years	M	ACM	<i>PKP2</i> c.1643delG p.Gly548ValfsX15
5	<i>PKP2</i> -5	36 years	M	ACM	<i>PKP2</i> c.2013delC p.Lys672ArgfsX12
6	Non- <i>PKP2</i> -1	29 years	W	ACM	No mutations in ACM-associated genes
7	Non- <i>PKP2</i> -2	70 years	M	ACM	No mutations in ACM-associated genes
8	Non- <i>PKP2</i> -3	52 years	M	ACM	No mutations in ACM-associated genes
9	Non- <i>PKP2</i> -4	46 years	M	MYO	-
10	Non- <i>PKP2</i> -5	69 years	M	Ischemia	-

ACM: arrhythmogenic cardiomyopathy; M: man, W: woman; MYO: myocarditis.

Supplementary Table S6. Characteristics of mice from which subcutaneous fat was taken, processed and analysed.

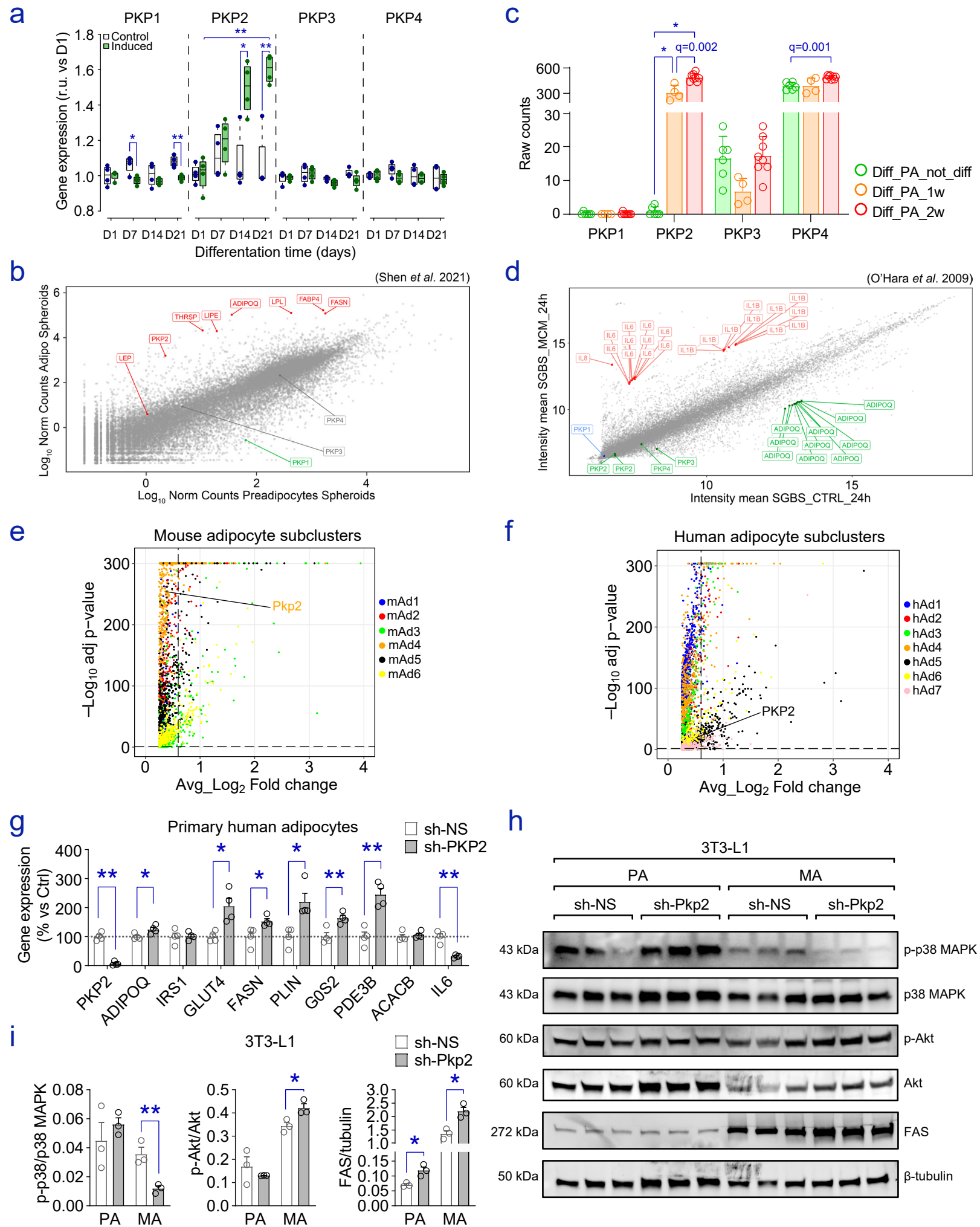
Genetics	Age	Sex
<i>Pkp2</i> ^{+/-} 1	5 months	F
<i>Pkp2</i> ^{+/-} 2	5 months	F
<i>Pkp2</i> ^{+/-} 3	3 months	M
<i>Pkp2</i> ^{+/-} 4	3 months	M
<i>Pkp2</i> ^{+/-} 5	3 months	M
Wt 1	5 months	F
Wt 2	5 months	F
Wt 3	5 months	F
Wt 4	3 months	M

M: male; F: female mice.

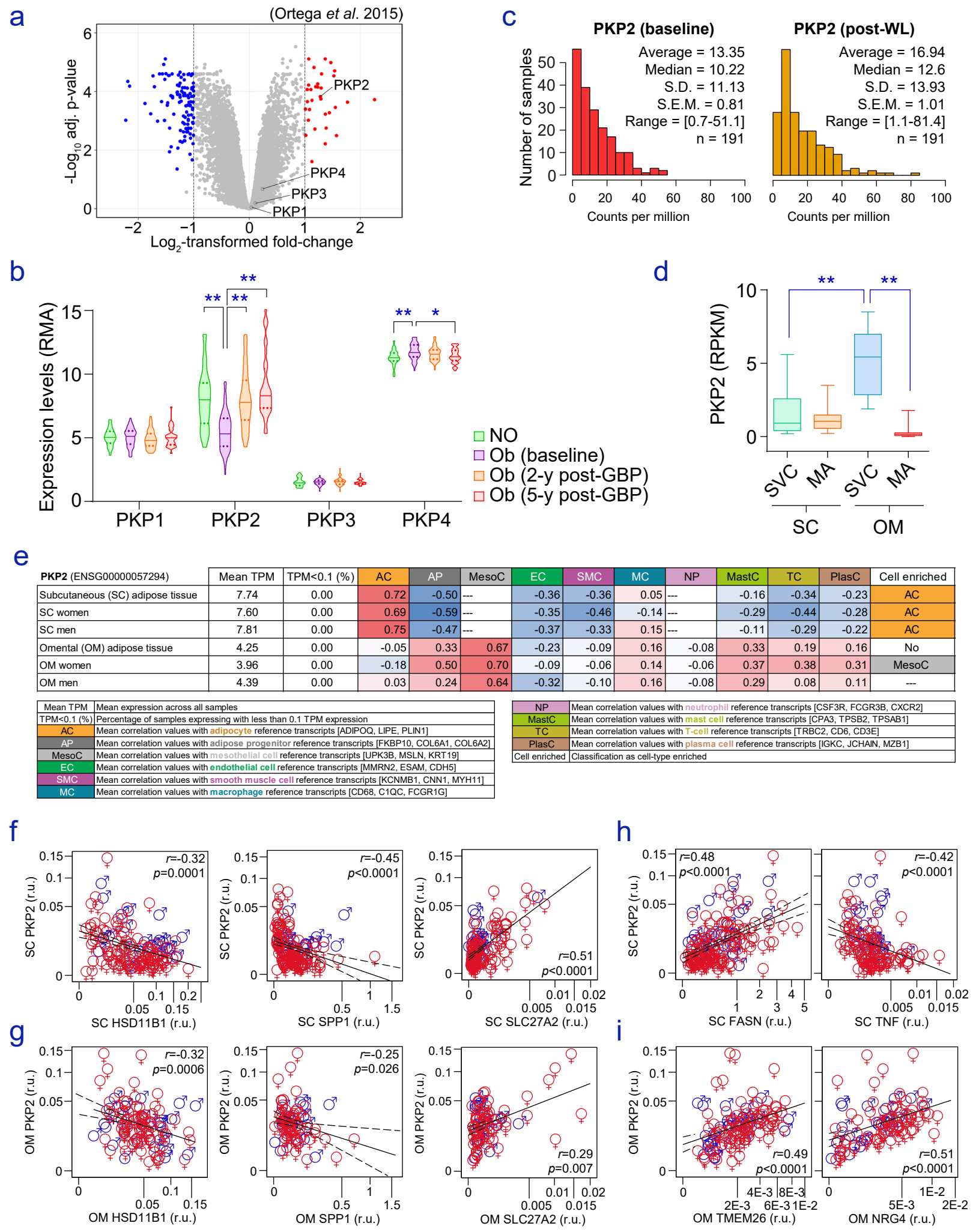
Supplementary Table S7. Paired SYBR Green primers and TaqMan assays used during this research.

Human genes	Forward SYBR Green primers	Reverse SYBR Green primers
<i>ACACB</i>	CTGAGTCACGTGCATATC	ACAAGTAGGCCTTGACAG
<i>AURKA</i>	CCTACAAAAGAATATCACGGG	CAAGTACTTCTCTGAGCATTG
<i>BAX</i>	AACTGGACAGTAACATGGAG	TTGCTGGCAAAGTAGAAAAG
<i>CCNB2</i>	ATTTTACAGGTTTCAGCCAG	ATCTCCTCATACTTGGGAAGC
<i>CCNE1</i>	AGACATACTTAAGGGATCAGC	CACACCTCCATTAACCAATC
<i>CDK1</i>	ACCTATGGAGTTGTGTATAAAG	GACTGACTATATTTGGATGACG
<i>CDK4</i>	AGAATCTACAGCTACCAGATG	AGAGTTTCCACAGAAGAGAG
<i>CDKN3</i>	GAAGAACTAAAGAGCTGTGG	TTCCATTATTTACAGCAGC
<i>CEBPA</i>	AGCCTTGTTTGTACTGTATG	AAAATGGTGGTTTAGCAGAG
<i>CREG1</i>	AGGAGAATCCATATGCTACAC	ATTATGTGAACACAAAGGGG
<i>DDIT4</i>	AATGTAAGAGTAGGAAGGGG	ACAGTTCTAGATGGAAGACC
<i>DEPDC1</i>	GAGGTCCTGATGATACATAC	TGCAGTCTGTAAGTAAGAGG
<i>DLGAP5</i>	CTCTAACTGTTTGGCATGAAG	TTTCTTCAAGTGATGGGAC
<i>ERF</i>	CAATTTCAACAACTGGTGC	AGGGAAGATGAAGATGAAGAG
<i>G0S2</i>	TGCCACTAAGGTCATTCC	TTCACCATCTTCCCCTTG
<i>HMGB1</i>	TACGAAAAGGATATTGCTGC	CTCCTCTTCCTTCTTTTCTTG
<i>HMGB2</i>	GAAAGCAGCTAAGCTAAAG	TTCATCTTCATCTCTTCCCTC
<i>IMPA2</i>	GATCATCAGAAAAGCCCTTAC	GTGATCTGTTTCTGTCAACAAG
<i>LMNB1</i>	AAAATTCTCAGGGAGAGGAG	TGGAAAAGTTCTTCTCAAC
<i>MKI67</i>	GACAGAGGTTCTTAAGAGAG	AACAATCAGATTTGCTTCCG
<i>MT1A</i>	AAATGCAAAGAGTGCAAATG	TTCTATATCTTCGAGCAGGG
<i>MT1F</i>	TCCAGATGTAACAGAGAG	AAAGGAATGTAGCAAATGGG
<i>PAPPA</i>	CATGGATCTAAATCTTGGCAG	TTTTGTATAATGCCATCGCC
<i>PDE3B</i>	AAATTCTGGAGGTGGAATG	ATACTCCGTAGAGAGGAAATG
<i>PLK4</i>	GTGGTGAGCATACTTGATTC	GTCTATCAGCAAGAGGAAAAC
<i>PPIA</i>	ATGGTTCACAGTTTTCATC	CTCCACAATATTCATGCCTTC
<i>SCD</i>	GCCCCTCTACTTGGGAAGACGA	AAGTGATCCCATACAGGGCTC
<i>SERPINE</i>	ATCCACAGCTGTCATAGTC	CACTTGGCCCATGAAAAG
<i>SLC39A3</i>	AGGGAAAAGCTCCAGAAG	GAAGACGGTCATGAAGAAG
<i>SPHK1</i>	TTCTTGAACCATTATGCTG	GATACTTCTCACTCTCTAGGTC
<i>SQSTM1</i>	TGTGAATTTCTGAAGAACG	TCGATATCAACTTCAATGCC
<i>TOP2A</i>	TCACAAGCAAGAAATCCAAG	ATCTTCATCTGACTCTTCCAG
Mouse genes	Forward SYBR Green primers	Reverse SYBR Green primers
<i>Acacb</i>	GCATGAAGGACATGTATGAG	AGGGATGTAGATGAGAATGG
<i>G0s2</i>	AGCTGAGGGGAAGAAGAAC	TATAGCTTCACTAGCTTCCC
<i>Pde3b</i>	AGGATTCTCAGTCAGGTTATG	GTTGTCAAATACCAAACAGC
<i>Ppia</i>	ACCAAACACAAACGGTTCCC	TCCCAAAGACCACATGCTTG

Human genes	Ref. # TaqMan assays	Mouse genes	Ref. # TaqMan assays
<i>ACLY</i>	Hs00982738_m1	<i>Adipoq</i>	Mm00456425_m1
<i>ADIPOQ</i>	Hs00605917_m1	<i>Fasn</i>	Mm00772290_m1
<i>CFB</i>	Hs00156060_m1	<i>Glut4</i>	Mm00436615_m1
<i>FASN</i>	Hs01005622_m1	<i>Il6</i>	Mm00446190_m1
<i>GLUT4</i>	Hs00168966_m1	<i>Irs1</i>	Mm01278327_m1
<i>HSD11B1</i>	Hs01547870_m1	<i>Pkp2</i>	Mm00503159_m1
<i>IL6</i>	Hs00985639_m1	<i>Plin1</i>	Mm00558672_m1
<i>IL8</i>	Hs00174103_m1	<i>Ppia</i>	Mm02342430_g1
<i>IRS1</i>	Hs00178563_m1		
<i>LEP</i>	Hs00174877_m1		
<i>NRG4</i>	Hs00945534_m1		
<i>PKP2</i>	Hs00428040_m1		
<i>PLIN1</i>	Hs00160173_m1		
<i>PPARG</i>	Hs01115513_m1		
<i>PPIA</i>	Hs99999904_m1		
<i>SLC27A2</i>	Hs00186324_m1		
<i>SPP1</i>	Hs00959010_m1		
<i>TMEM26</i>	Hs00415619_m1		
<i>TNF</i>	Hs00174128_m1		

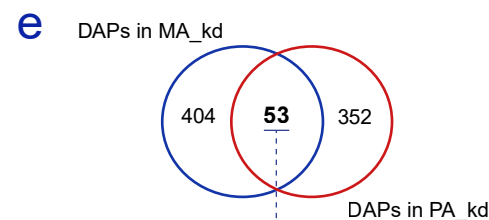
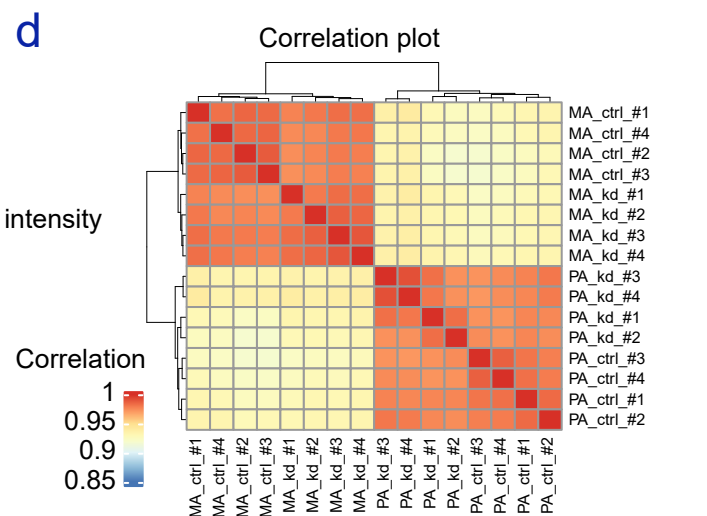
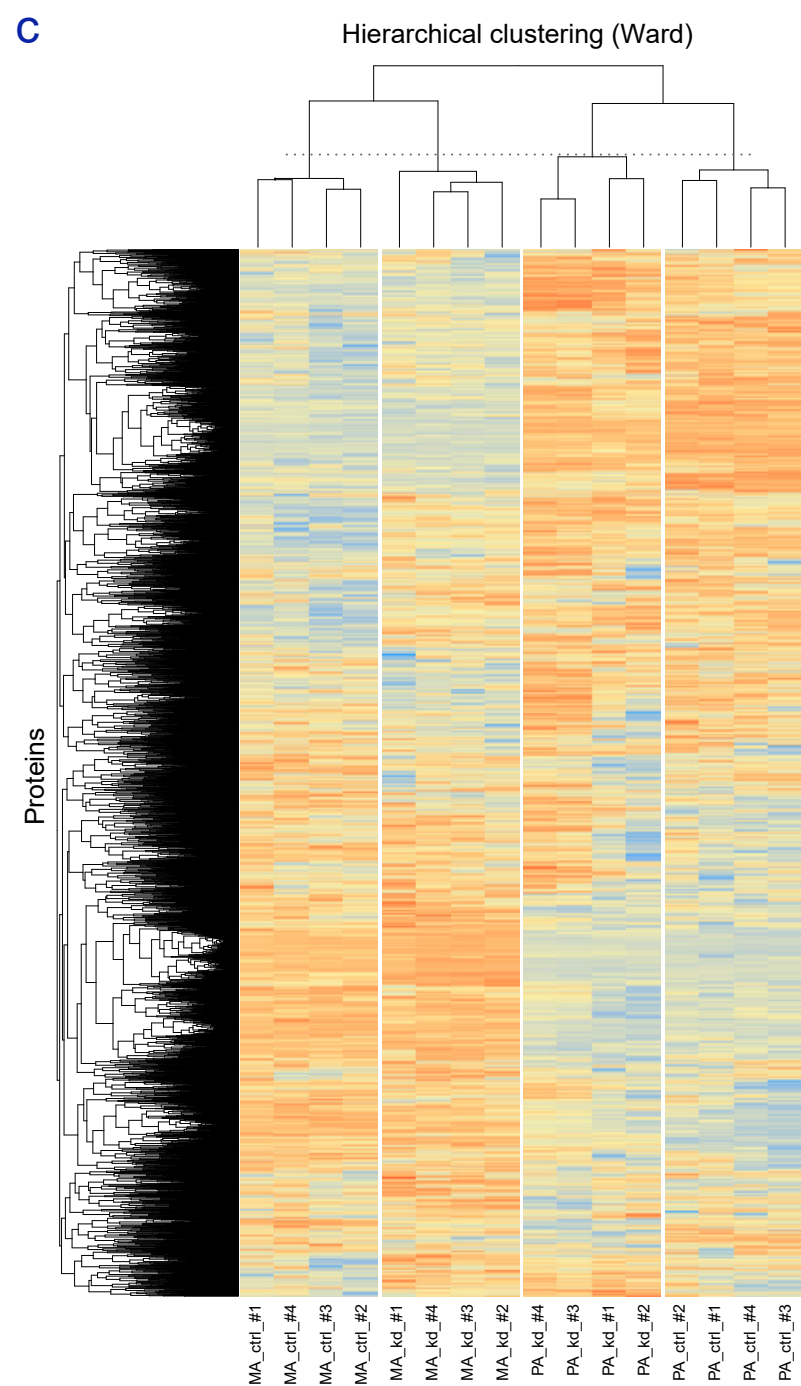
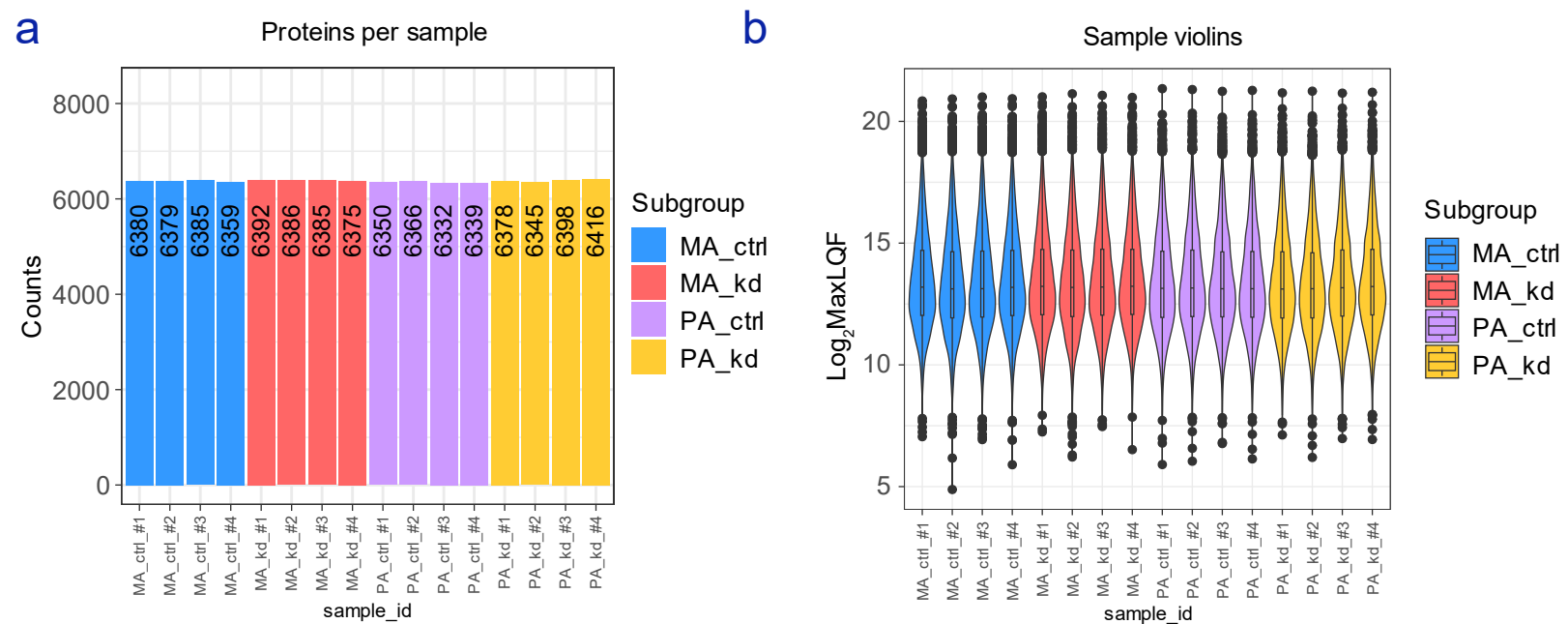


Supplementary Figure S1. (a) Plakophilin 1 to 4 (*PKP1-4*) in human fat precursor cells when induced to differentiate into adipocytes (n=4 biological replicates/group/timepoint)¹. The black line inside the box shows the median, and the size of the box is determined by the 25th and 75th percentiles, while whiskers indicate the maximum and minimum values. (b) The scatter plot uses dots to compare gene expression values (Log₁₀ normalized counts) in human preadipocytes and differentiated adipocyte spheroids². Adipocyte biomarkers and *PKP1-4* are labelled in red (increased), green (decreased), or grey (no significant variations). (c) Raw counts (RNA-seq) for each plakophilin in 2D cultures of human preadipocytes (PA) under the influence of adipogenic conditions for 1 and 2 weeks (w)². This plot shows the mean + S.E.M of n=6, 4, and 8 biological replicates for days 0, 7, and 14 of hormonal stimuli, respectively. *q<0.001 when comparisons were analyzed individually using the two-stage linear step-up procedure of Benjamini, Krieger and Yekutieli, with Q=1%, and without assuming a consistent S.D. (d) Expression of transcripts coding for *PKP1-4*, adiponectin (*ADIPOQ*), and pro-inflammatory adipose-related interleukins (*IL6*, *8* and *1β*) in SGBS-derived adipocytes challenged with 14% macrophage lipopolysaccharide (LPS)-conditioned media (MCM) for 24 h³. Red ink in labels depicts increased levels, and green labels show transcripts significantly decreased in inflamed adipocytes. Expression of *PKP2* (but none of the others plakophilins) was confirmed in (e) mouse (mAd4) and (f) human (hAd5) adipocyte subpopulations in the single-cell atlas of Emont *et al.*⁴. There, they compared the percentage of cells in the cluster where the gene is detected versus the percentage of cells on average in all the other clusters (Avg_Log₂ Fold-change). (g) Adipocyte biomarkers in differentiated human adipocytes treated with lentivirals (sh)RNAs against *PKP2* (mean + S.E.M; n=4/group). (h-i) Western plots show decreased p-p38/p38 MAPK (inflammation), and increased metabolic performance (p-Akt/Akt and FAS) in retrovirally transfected 3T3-L1 preadipocytes (PA) and mature adipocytes (MA) with diminished *PKP2* (sh-Pkp2), as compared to NS controls (mean + S.E.M; n=3/group). The statistical significance for each comparison was determined by two-tailed Fisher's exact t-test. *p<0.05; **p<0.01.

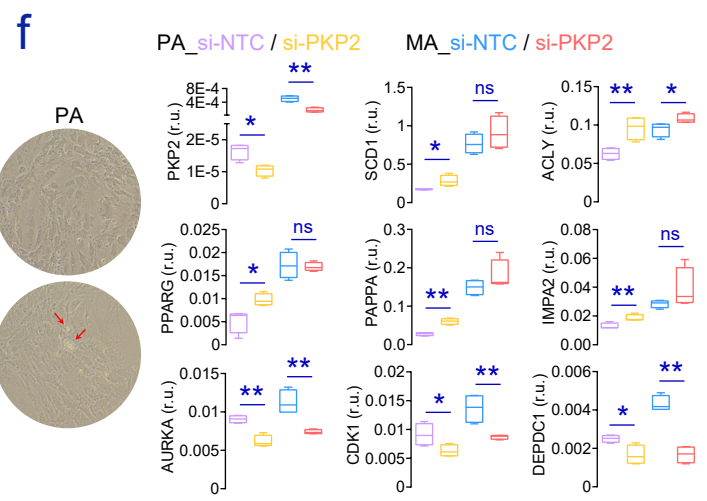


Supplementary Figure S2. (a) The Volcano shows expression dynamics for plakophilins 1 to 4 (*PKP1-4*) in subcutaneous (SC) adipose tissue after significant weight loss ⁵. (b) Also in ⁶, when we checked expression of SC *PKP1-4* in participants with obesity (Ob) and sex and age-matched non-obese (NO) subjects (n=28), or in the former when compared to the expression levels post-2 (n=49) and 5 (n=38) years after gastric bypass (GBP), only *PKP2* displayed a significant increase. (c) *PKP2* counts per million in samples of SC human adipose tissue before (baseline) and after diet-induced weight loss (post-WL) ⁷. (d) *PKP2* gene expression levels (RPKM) in the single-cell RNA-seq of mature adipocytes (MA) and the stromal vascular cell (SVC) fraction of SC and omental (OM) adipose tissue samples ⁸ (see also our own results in [Figure 2i](#)). The coloured line inside the boxplot represent the median value, and the size of the box is determined by the 25th and 75th percentile, while the whiskers represents the maximum and minimum values. Statistics were performed using two-sided Student t-tests, and *p<0.05 and **p<0.001 in each dataset. (e) Mean TPM (transcript per million), detectability (TPM>0.1%), and heat map of pairwise Spearman correlation coefficients for *PKP2* (ENSG00000057294) and reference genes for different populations of adipose tissue resident cells. The lack of values for mesothelial cells (MesoC) and neutrophils (NP) in SC adipose tissue is due to the low number/absence of these cell types in this fat depot, as explained in ⁹. Scatter plots show the association of 11 β -hydroxysteroid dehydrogenase type 1 (*HSD11B1*), osteopontin (*SPP1*) and solute carrier family 27 (fatty acid transporter), member 2 (*SLC27A2*) with *PKP2* in (f) SC and (g) OM depots of fat (RT-PCR), and also between (h) SC *PKP2* and *FASN* (adipogenesis) and *TNF* (inflammation), and between (i) OM *PKP2* and the expression of *NRG4* and *TMEM26*. Two-sided Spearman's rank correlation coefficients (*r*) and p-values are provided for each association (see in the supplementary [Table S3](#) and in the [Source Data file](#) provided with this article). Men (blue) and women (red) are depicted in gender glyphs.

Supplementary Figure S3. (a) Enriched terms, (b) Gene Ontology (GO) pathways, and (c) Ingenuity Pathway Analysis (IPA) of changes observed in human adipocytes with diminished *PKP2* levels lasting 3 (si-*PKP2*) or 6 (sh-*PKP2*) days. The interpretation of lists of genes showing significant variations ($FDR < 0.05$) was also performed by means of the Gene Set Enrichment Analysis (GSEA) software, based on the Hallmark gene set to depict the weight, enrichment score (ES) and profile of genes related to the biological pathways most significantly downregulated during assays lasting either (d) 6 or (e) 3 days. Venn diagrams summarize the overlap between treatments for (f) each hallmark and (g) merged E2F targets and genes involved in the G2/M checkpoint with significant variation in both experimental approaches (see also the dots inked in colours in [Figure 3c](#)).

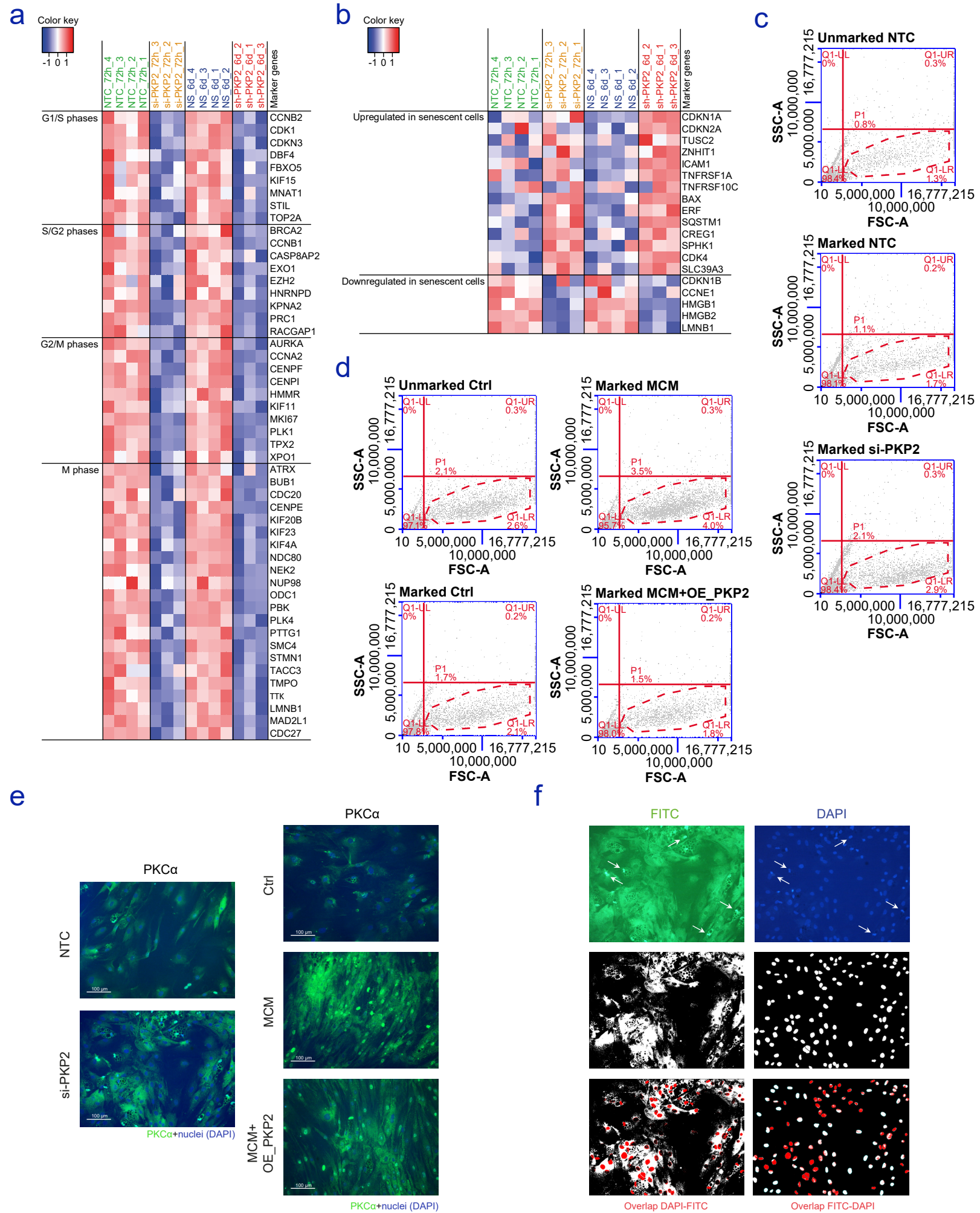


LPP, ITSN1, NAV1, ACLY, RBM3, EPS8, PDLIM2, PLEKH45, CEP41, PALLD, MAP1LC3B, MAP1LC3B2, SH3D19, PAWR, SORBS2, MRR1, DEPTOR, GALNT5, GSE1, ATP9A, NPR3, CAAP1, IGFBP3, CYP51A1, SCD, ABHD4, PTBP2, OAS3, GBP1, GBP2, HLA-F, MT1F, UROD, AIDA, TFB1M, INO80, PTX3, CFB, SERPINB2, STAT2, KIDINS220, ITIH2, B2M, PRRC2C, UAP1, KPNA2, PDGFRB, CPNE1, GMPS, COA4, ZNF385A, SELENOO, KIF23, NTM, LOXL3.



Supplementary Figure S4. (a) Raw numbers of identified proteins in each cell sample studied by quantitative proteomics and in-depth proteome-wide analysis, after filtering out peptides without replication within subgroups and proteins with less than 1 peptide. Intensities of proteins in a \log_2 scale are plotted on (b) for each biological replicate and group. (c) Hierarchical clustering of proteins abundance (in rows) for each sample (in columns). (d) The cluster heatmap shows Pearson correlation coefficients between assessed protein samples. (e) The Venn diagram indicates the number of DAPs with $FDR < 0.05$ in common for MA_kd and PA_kd (6.6% of total), which are listed below in red (increased in both), green (decreased in both), purple (increased in MA, decreased in PA), and orange (decreased in MA, increased in PA). (f) A few lipid vacuoles were apparent in the cytoplasm of si-PKP2-targeted undifferentiated PA, together with gene expression patterns reminiscent of an adipocyte-like phenotype. Box plots show the median and 25th and 75th percentiles in boxes, and whiskers that indicate the maximum and minimum values for each group (n=4/group). Statistical significance was assessed by two-tailed Fisher's exact t-test, and no adjustments were made for multiple comparisons. r.u., relative units; ns, not significant; * $p < 0.05$; ** $p < 0.01$.

Supplementary Figure S5. Manhattan plot of significant (adjusted p-value<0.05) gene set enrichment results mapped by means of the g:Profiler tool g:GOST (<https://biit.cs.ut.ee/gprofiler/gost>) on our lists of proteins (a) down and (b) upregulated in si-PKP2 adipocytes, and (c) down and (d) upregulated in si-PKP2 preadipocytes, as compared to control. Some of the most relevant terms in Gene Ontology (GO) enrichment database are labelled with reference numbers further depicted in the supplementary [Table S4](#).



Supplementary Figure S6. Heatmaps of microarray data showing (a) cell cycle-specific and (b) senescence-associated gene expression patterns in human adipocytes with impaired PKP2 levels lasting 3 (si-PKP2) or 6 (sh-PKP2) days and respective controls. Scatter dot plots show randomly selected images and percent of senescence-associated β -galactosidase (SA- β -gal) active adipocytes under (c) siRNA-mediated PKP2 silencing, and (d) responding to MCM and complemented with a plasmid coding for PKP2 (OE_PKP2), as provided by a BD Accuri C6 flow cytometer (see also in [Figure 6e](#)). S/FSC stands for side/forward scatter measures. Below, (e) randomly selected 20x immunofluorescent images show the (f) staining of PKC α (FITC-green) in adipocytes' nuclei (DAPI-blue signal). Results assessed by means of this approach are represented as % overlap in [Figure 6i](#), and show results assessed in one experiment (n=4 biological replicates/group).

REFERENCES

1. Ambele, M. A., Dessels, C., Durandt, C. & Pepper, M. S. Genome-wide analysis of gene expression during adipogenesis in human adipose-derived stromal cells reveals novel patterns of gene expression during adipocyte differentiation. *Stem Cell Res.* **16**, 725–734 (2016).
2. Shen, J. X. *et al.* 3D Adipose Tissue Culture Links the Organotypic Microenvironment to Improved Adipogenesis. *Adv. Sci. (Weinheim, Baden-Wurttemberg, Ger.)* **8**, e2100106 (2021).
3. O’Hara, A., Lim, F. L., Mazzatti, D. J. & Trayhurn, P. Microarray analysis identifies matrix metalloproteinases (MMPs) as key genes whose expression is up-regulated in human adipocytes by macrophage-conditioned medium. *Pflugers Arch. Eur. J. Physiol.* **458**, 725–734 (2009).
4. Emont, M. P. *et al.* A single-cell atlas of human and mouse white adipose tissue. *Nature* **603**, 1103–1114 (2022).
5. Ortega, F. J. *et al.* Surgery-induced weight loss is associated with the downregulation of genes targeted by MicroRNAs in adipose tissue. *J. Clin. Endocrinol. Metab.* **100**, E1467–E1476 (2015).
6. Kerr, A. G., Andersson, D. P., Rydén, M., Arner, P. & Dahlman, I. Long-term changes in adipose tissue gene expression following bariatric surgery. *J. Intern. Med.* **288**, 219–233 (2020).
7. Larsen, T. M. *et al.* Diets with high or low protein content and glycemic index for weight-loss maintenance. *N. Engl. J. Med.* **363**, 2102–2113 (2010).
8. Vijay, J. *et al.* Single-cell analysis of human adipose tissue identifies depot and disease specific cell types. *Nat. Metab.* **2**, 97–109 (2020).
9. Norreen-Thorsen, M. *et al.* A human adipose tissue cell-type transcriptome atlas. *Cell Rep.* **40**, 111046 (2022).